



TECHNOLOGY DEVELOPMENT CENTER NEWS

NATIONAL INSTITUTE OF INFORMATION AND
COMMUNICATIONS TECHNOLOGY

Serial No. 24

July 2004



CONTENTS

Technical Reports

- Rapid UT1-UTC estimation from Westford-Kashima e-VLBI experiment (2) 2**
Yasuhiro Koyama, Tetsuro Kondo, Hiroshi Takeuchi, Masaki Hirabaru, David Lapsley, Kevin Dudevoir, and Alan Whitney
- HAYABUSA VLBI observations for development of deep space tracking – Preliminary report – 7**
Ryuichi Ichikawa, Mamoru Sekido, Hiro Osaki, Yasuhiro Koyama, Tetsuro Kondo, Makoto Yoshikawa, and VLBI spacecraft tracking group
- Development of software baseband converter 9**
Hiroshi Takeuchi
- Derivation of relativistic VLBI delay model for finite distance radio source (Part I) 11**
Mamoru Sekido and Toshio Fukushima
- The Australian experience with the PC-EVN recorder 18**
Dodson, R., S. Tingay, C. West, A. Hotan, C. Phillips, J. Ritakari, F. Briggs, G. Torr, J. Quick, Y. Koyama, W. Brisken, B. Reid, and D. Lewis

- News - News - News - News -

- CARAVAN-35, small radio telescope package released 23**

Announcement

- 3rd e-VLBI Workshop 6**

Rapid UT1-UTC estimation from Westford-Kashima e-VLBI experiment (2)

Yasuhiro Koyama¹ (koyama@nict.go.jp),
Tetsuro Kondo¹, Hiroshi Takeuchi¹, Masaki Hirabaru², David Lapsley³, Kevin Dudevoir³, and Alan Whitney³

¹ *Kashima Space Research Center, National Institute of Information and Communications Technology, 893-1 Hirai, Kashima, Ibaraki 314-8501, Japan*

² *Koganei Headquarters, National Institute of Information and Communications Technology*

³ *Haystack Observatory, Massachusetts Institute of Technology*

1. Introduction

After the previous report [Koyama, et al., 2003a], a test e-VLBI session was performed on June 27 with the baseline between Kashima 34m station and Westford 18m station to demonstrate the rapid UT1-UTC estimation from the actual observations. The observations were performed for about two hours at the total effective data rate of 56Mbps, and the data were processed using both Mark-4 correlator at Haystack Observatory and K5 software correlator at Kashima. By using the K5 correlator outputs, UT1-UTC was estimated at about 21 hours 20 minutes after the last observa-

tion completed [Koyama, et al., 2003b). Following this successful demonstration of e-VLBI technique to determine UT1-UTC value so rapidly, Observing Program Committee of the IVS started to discuss the possibility to introduce the e-VLBI technique to the routine international VLBI sessions coordinated by IVS. The capability of the rapid UT1-UTC estimation is considered to be best utilized by the single baseline intensive sessions and it was recommended to try to establish routine e-VLBI session series every Sunday. Currently, the intensive sessions are performed by using a baseline between Kokee Park and Wettzell stations on weekdays (from Monday through Friday), and by using a baseline between Wettzell and Tsukuba stations on Saturdays. By filling the vacant Sundays by using the e-VLBI intensive sessions, daily monitoring of UT1-UTC will be realized and it was considered to be the best way to introduce the e-VLBI in the regular session. If these e-VLBI sessions are considered to be smooth and reliable, efforts will follow to make the e-VLBI becomes possible for the existing intensive sessions to improve the latency of the UT1-UTC estimation. In this scope, we have performed two e-VLBI sessions again by the baseline between Westford and Kashima 34m stations to prepare the necessary softwares to establish the routine e-VLBI intensive sessions. In this report, we will describe the recent developments to improve the software correlations and the network connectivities and will discuss about the results obtained by the test sessions.

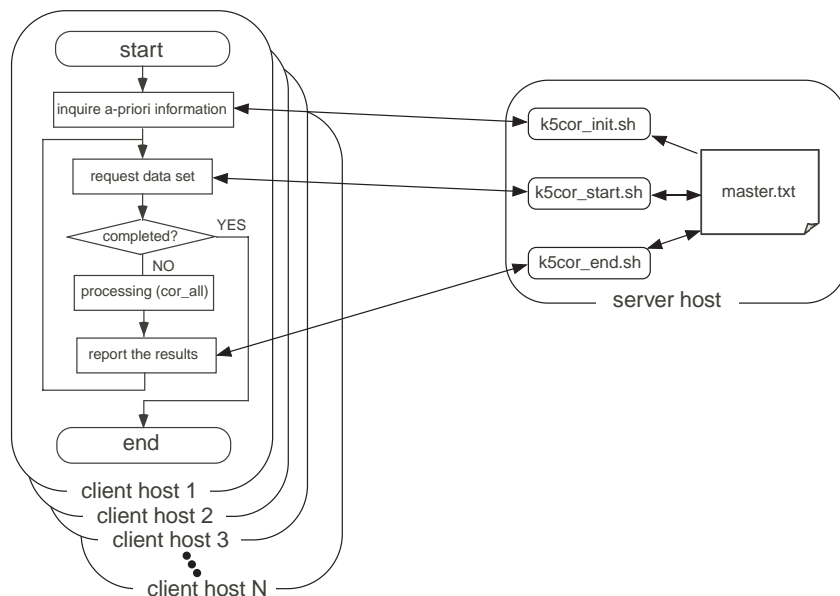


Figure 1. A schematic diagram of the server and client mechanism developed for the distributed cross correlation processing.

2. Developments of the K5 Software Correlator

After the test e-VLBI sessions in 2003, the software correlation programs for the K5 software correlator have been improved for their processing speed [Kondo, *et al.*, 2003]. The previous version of the software correlation program processes the FFT processing first and then calculate the cross correlation spectrum to obtain cross correlation function. The fast version of the software correlation program uses the XF algorithm, where the cross correlation function is calculated directly from the observation raw data. The processing speed was improved by a factor of about 6.2. With the lag length of 32, 8MHz sampling data can be processed at about the same speed of the recording speed by using an 1GHz Pentium 4 CPU. In addition, efforts have been made to realize distributed processing by using multiple CPUs. One of the efforts is to utilize unused CPU powers of the conventional PC systems by developing a screen saver program to download the data files from a server and perform the software correlation [Takeuchi, *et al.*, 2004]. The mechanism, which we are calling as VLBI@home, is consisted by a screen saver program and a server system program. The server system program processes the requests from the clients systems running the screen saver program. Currently, the screen saver program has been developed on the Microsoft Windows operating platforms. Any PCs connected to the Internet can be used as the clients. Once the screen saver program is installed, the program begins to communicate with the server program over the Internet and begin to download the data files and then perform the correlation processing. Once the processing completes, the results will be reported to the server program and then the client system begins to process the next data set. If the user of the PC system starts to use the CPU for the other purposes, the screen saver program promptly terminates the processing but the processing can be resumed later when the CPU is not used for a certain time specified by the screen saver configuration.

In addition to the VLBI@home programs, a simple server and client mechanism shown in Figure 1 has also been developed by using simple shell scripts and a few Fortran programs. On the server system, a master control file 'master.txt' is maintained and the file holds all the information necessary to control the distributed processing. By reading the master control file, the server system can assign a set of data files with which the client systems can process. Each client system obtains the data files and necessary information from the server system and starts to process the data. When

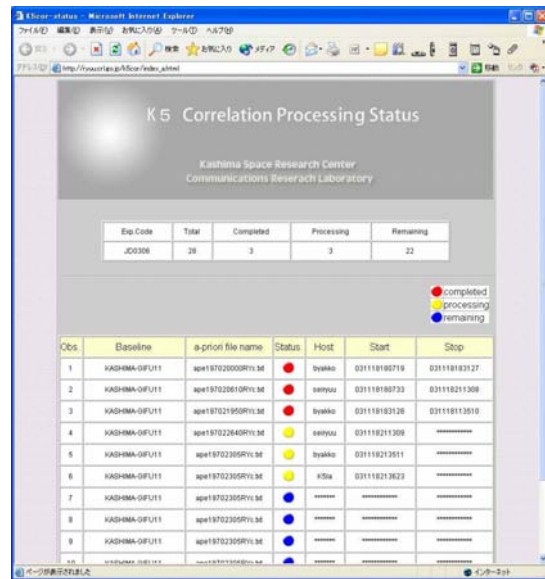


Figure 2. A WWW browser screen for monitoring distributed processing status under developments.

the processing is completed at the client system, the client system places the results to a specific place and then requests the server system for the next data files. By using this simple mechanism, all the data files can be processed effectively using available computing resources of the client PC systems. Although the performance of each PC system may differ, each client PC systems can process the data files according to the available performance. Status monitoring capability is also under developments as shown in Figure 2. Any WWW browsers will be able to show the current status how the distributed processing is on going. In this server and client mechanism, data files are accessed by using the Network File Server (NFS) protocol. The disks where the data files are located are mutually mounted by multiple Linux and Free BSD unix servers by using amd (Auto Mount Daemon) or autofs programs. The processed results are written onto a single disk which is also mounted by the NFS from the clients. To avoid multiple access to the master control file, the server system creates a empty file when it starts to process the master control file to prevent the other processes to access the file. After the modifications to the master control file, the empty file is erased and the other processes is allowed to process the file. In this way, the client systems can process the correlation processing independently without the tight control from the server system. This mechanism is very simple but it works very well even when the performance of the client systems are very different. The mas-

ter control file contains information when the job is started by which client system and can reset the status when the results are not reported within a specified timeout time. By doing this, the client program can start or stop at any time.

3. Improvements of the Network Connectivities

After the test e-VLBI sessions in 2003, the GALAXY network connection to the Kashima Space Research Center was terminated. The GALAXY network is a high speed dedicated research network for e-VLBI coordinated by the collaborations among NICT, NTT Laboratories, National Astronomical Observatory, and Japan Aerospace Exploration Agency [Uose, *et al.*, 2003]. Before the termination of the connection, Kashima and Musashino R&D Center of the NTT Laboratories used to be connected by the OC-48 ATM network and GbE Ethernet was supported over the ATM network. The TCP/IP connection was then routed to the Abilene network in the United States via the GEMnet network coordinated by the NTT Laboratories. The connection was used for the two test e-VLBI sessions in 2003.

Since the GALAXY connection to Kashima was terminated in 2003, the institutional LAN connection inside NICT between Kashima and Koganei headquarters had been only available for the e-VLBI data transfer from the stations at Kashima. The connection between Kashima and Koganei has the maximum bandwidth of 100Mbps and the network is shared by many traffic form the various purposes among many projects of the NICT. By using this connection, we started to record all of the observation data for the IVS geodetic VLBI sessions at Kashima 34m station with the K5 system since October 2003, and to transfer K5 data files to the server at Haystack Observatory or in Washington D. C. and then used for correlation processing after converting the data file format to the Mark-5 system [Koyama *et al.*, 2003c]. The typical data transfer rate was about 30Mbps after tuning various network parameters and using multiple TCP/IP connections by using *bbftp* program.

On the other hand, an independent high speed research network in Japan based on ATM used to be operated by Telecommunications Advancement Organization (TAO) to support advanced research and developments for the communications technology. The network was called Japan Gigabit Network (JGN) and it supported many research projects. In April 2004, the TAO and Communications Research Laboratory were merged and the new institute was established as NICT. At the same time, the JGN network was upgrade and the new

research test-bed network Japan Gigabit Network II (JGNII) was established based on the TCP/IP network. As shown in the Figure 3, Kashima and Koganei was connected by the OC-192 (2.4Gbps) connection and the GbE TCP/IP connection was established between these sites. The TCP/IP network is then routed to the Abilene network in the United States via JGNII/TransPAC network. As shown in Figure 4, the connection between JGNII and the Abilene was recently upgrade to two lines of OC-48 connections.

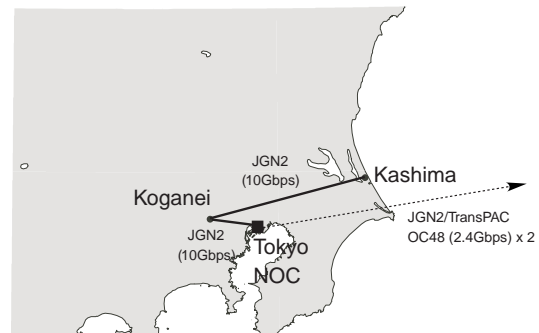


Figure 3. Configuration of the high speed network in Japan.

4. Experiments

As explained in the Introduction, two test e-VLBI session were performed in June 2004. The first session was performed for about two hours from 19:00 UT on June 22. The purpose of the first session is to use it as a rehearsal. By processing the observed data in the first session, it was estimated that one hour of observations would be enough to estimate UT1-UTC with the uncertainty of 20 microsec. Therefore, the second session was performed for about one hour. After the observations, the data recorded at Westford station with the Mark-5 system were extracted and transferred to Kashima through Abilene/TransPAC/JGNII networks. 13.5 GBytes of data were transferred in about 1 hour and 15 minutes and the average data transfer rate was 24 Mbps. The transferred data were then converted to the K5 file format. During the one hour session, 18 scans were recorded in total. 13 scans were assigned to the NFS based distributed software correlation using 12 CPUs running on Linux and FreeBSD. The remaining 5 scans were assigned to VLBI@home and 9 CPUs were used. As soon as the data format conversion completed, the software correlation was started. At this point, the network connection at Kashima became unstable and the data access became very

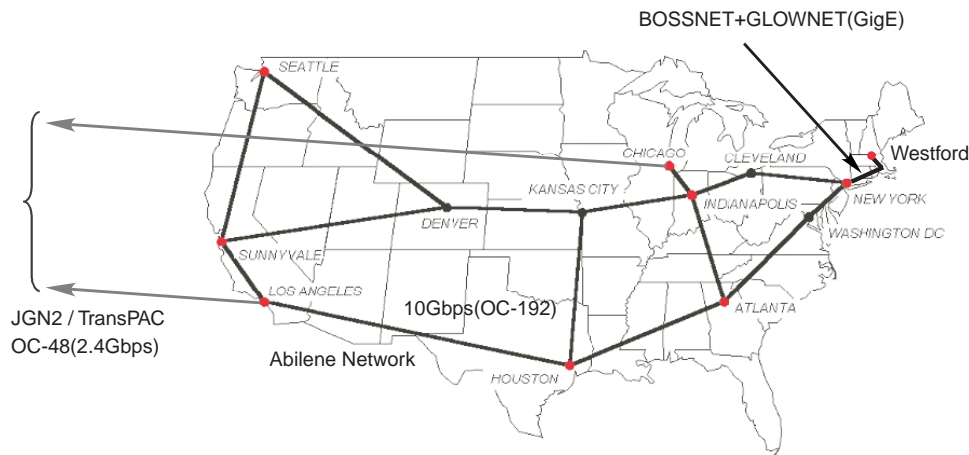


Figure 4. Configuration of the high speed network in the United States.

slow. To solve this problem, the servers were rebooted a few times and these operations caused the unexpected delay of the processing. As the results, it took about 2 hours and 38 minutes. Immediately after all the correlation processing completed, database files were generated and the data analysis was performed by using CALC and SOLVE softwares developed by the Goddard Space Flight Center of NASA. The data analysis was completed at 4 hours and 30 minutes after the last observation in the session completed. Table 1 shows the time sequence from the observations

Table 1. Time sequence from observations through the data analysis of the e-VLBI session on June 29, 2004

Events	Time in UT (Date)
Observing session started	19:00 (June 29)
Observing session finished	20:00
File transfer started	20:13
File transfer completed	21:28
Correlation processing completed	00:16 (June 30)
Data analysis completed	00:30

For both of the two test e-VLBI sessions, effective data rate was 56Mbps. Frequency bandwidth for each channel was 2MHz. For X-band, 8 channels were used while the remaining 6 channels were used for S-band. In the data analysis, atmospheric delay and clock offset were estimated as well as the UT1-UTC. The formal uncertainty of the UT1-UTC estimation was 22.0 microsec.

5. Conclusions and Future Plans

In conclusion, the capability of estimating UT1-UTC from one baseline e-VLBI session was success-

fully demonstrated from the actual test e-VLBI session. After the demonstration, the distributed software correlations were performed for a few times with the same condition, but the network problem which caused the delay did not occur again. If the problem did not occur, the software correlation processing would have been completed within 30 minutes. Therefore, it will be possible to estimate UT1-UTC from the similar test session within 3 hours from the last observation, since it took about 1.5 hours to solve the problem. During the test e-VLBI sessions in June 2004, many procedures were still performed manually while many procedures have been automated. But the situation will improve as the software developments advance. The network connection from the Westford station of the Haystack Observatory to the Abilene network will be upgraded in near future. Tsukuba station has already been connected to the high speed network and the Geographical Survey Institute has participated in the regular IVS sessions with the K5 system since May 2004. To connect the network, 2.4Gbps ATM link between Tsukuba and NTT Musashino R&D Center operated as the GALAXY network is used and TCP/IP interface is used to allow GbE TCP/IP data transfer. At present, TCP/IP connection is only possible when the other purposes do not use the ATM connection, but there is a plan to improve the situation by using an ATM switch at Tsukuba station. Onsala and Wettzell stations also have capability to perform e-VLBI operation by using the Mark-5 systems and the good network connectivity situations. Therefore, it will be possible to start e-VLBI intensive sessions by using Tsukuba station and one station from Wettzell, Westford, and Onsala stations. Also at present, discussions about the stan-

standard mechanism of the e-VLBI data transfer is under discussion. By standardizing the data transfer mechanism, the file conversion processing will become unnecessary and we can expect to improve the latency.

Acknowledgment: The authors would like to appreciate many members of the Haystack Observatory and NICT for supporting the e-VLBI developments and observations. Research partners at the NTT Communications Corporation, KDDI R&D Laboratories, NTT Laboratories, JGNII, Internet2 have made the e-VLBI session possible together. e-VLBI research and developments in Japan have been promoted by a close collaboration among NICT, Geographical Survey Institute, NTT Laboratories, National Astronomical Observatory, Japan Aerospace Exploration Agency, Gifu University and Yamaguchi University.

References

- Kondo, T., Y. Koyama, and H. Osaki (2003), Current Status of the K5 Software Correlator for Geodetic VLBI, IVS CRL-TDC News, No. 23, pp. 18–20.
- Koyama, Y., T. Kondo, H. Osaki (2003a), Rapid UT1-UTC estimation from Westford-Kashima e-VLBI experiment, IVS CRL-TDC News, No. 22, pp. 6–9.
- Koyama, Y., T. Kondo, H. Osaki, A. Whitney, and K. Dudevoir (2003b), Rapid turn around EOP measurements by VLBI over the Internet, in Proceedings of the IAG G02 Symposium in the 23rd. IUGG General Assembly, Sapporo Japan, July 2003 (*in printing*).
- Takeuchi, H., T. Kondo, Y. Koyama, and J. Nakajima (2004), VLBI@home - VLBI Correlator by GRID Computing System, in International VLBI Service for Geodesy and Astrometry 2004 General Meeting Proceedings, eds. N. R. Vandenberg and K. D. Baver, NASA/CP-2004-212255 (*in printing*).
- Uose, H. (2003), Application of Ultrahigh-speed Network to Advanced Science, NTT Technical Review, Vol. 1, No.5, pp.39–47
-

3rd e-VLBI Workshop October 6-7, 2004 Makuhari, Japan



Logo designed by S. Arimura
and Y. Koyama

hosted by
**National Institute of Information and
Communications Technology**

Objectives: The 1st e-VLBI workshop was held at MIT Haystack Observatory in April 2002. The purpose of the workshop was to promote global real-time and near-real-time VLBI observations using the high speed network infrastructure, and it made a great success. Following the success, the 2nd e-VLBI workshop was held at Joint Institute for VLBI in Europe (JIVE) in May 2003 and enormous progress was seen both in the network infrastructure and the e-VLBI observations and processing systems. The 3rd e-VLBI workshop is expected to present an ideal opportunity to further enhance and accelerate the e-VLBI research and developments, again.

Topics to be discussed will include:

- Reports on e-VLBI tests and demonstrations
- Plans for ongoing e-VLBI development
- Status of interaction with network providers and developers
- International networking facilities - now and future
- Standards and protocols for e-VLBI data transfer.
- Hardware and software interfaces to telescope back-ends and correlators
- Related projects

More information is available on Web Site
“<http://www.nict.go.jp/ka/radioastro/evlbi2004/index.html>”.

HAYABUSA VLBI Observations for Development of Deep Space Tracking –Preliminary Report–

Ryuichi Ichikawa¹ (*richi@nict.go.jp*), Mamoru Sekido¹, Hiro Osaki, Yasuhiro Koyama¹, Tetsuro Kondo¹, Makoto Yoshikawa², and VLBI spacecraft tracking group³

¹*Kashima Space Research Center
National Institute of Information and
Communications Technology
893-1 Hirai, Kashima, Ibaraki 314-8501, Japan*

²*Institute of Space and Astronautical Science,
Japan Aerospace Exploration Agency*

³*JAXA, GSI, NAO, Hokkaido Univ., Gifu Univ.,
Yamaguchi Univ.*

The precise and realtime navigation of the interplanetary spacecrafts using VLBI technique is currently under development at NICT (National Institute of Information and Communications [former CRL]). We performed more than 30 VLBI experiments for the Japan's NOZOMI Mars probe from September 2002 until June 2003 [Ichikawa *et al.*, 2003; Sekido *et al.*, 2003]. The fringe products of group delays were successfully detected from these VLBI experiments in spite of weak and narrow-bandwidth NOZOMI signal. The group delays were used to validate the operational orbit determination based on the range and range rate (R&RR) data sets by ISAS (Institute of Space and Astronautical Science).

Though the rms scatter of the group delays of VLBI data from the R&RR results are relatively large up to several tens nanoseconds, the both results are consistent with each other. We also detected phase delay fringes using updated correlation software [Sekido *et al.*, 2003]. The estimated position based on the phase delays are good consistent with the R&RR results. In particular, the declinations determined by phase delay signals are identical with those obtained by R&RR values. Unfortunately, ISAS scientists gave up to inject the NOZOMI into orbit around Mars due to unrecoverable malfunction on December 9, 2003.

We perform another VLBI experiments for tracking of HAYABUSA spacecraft. HAYABUSA, which means "Falcon" in Japanese, was launched on May 9 2003, and has been flying steadily towards an asteroid named "Itokawa", after the late Dr. Hideo Itokawa, the father of Japan's space development program. HAYABUSA is traveling through space using an ion engine. It will orbit the asteroid, land on it, and bring back a sample from its surface [JAXA, 2003].

The first HAYABUSA VLBI experiment was performed at X-band(8.4 GHz) using six VLBI stations in Japan on November 26, 2003. We used the "K5 VLBI system [Kondo *et al.*, 2003]" to acquire the VLBI data at the stations. Figure 1 shows two examples of group delay fringes of HAYABUSA range and telemetry signals for the Kashima-Usuda baseline. According to the comparison between group delays and R&RR results, large residuals more than 100 nanoseconds are represented as shown in Figure 2.

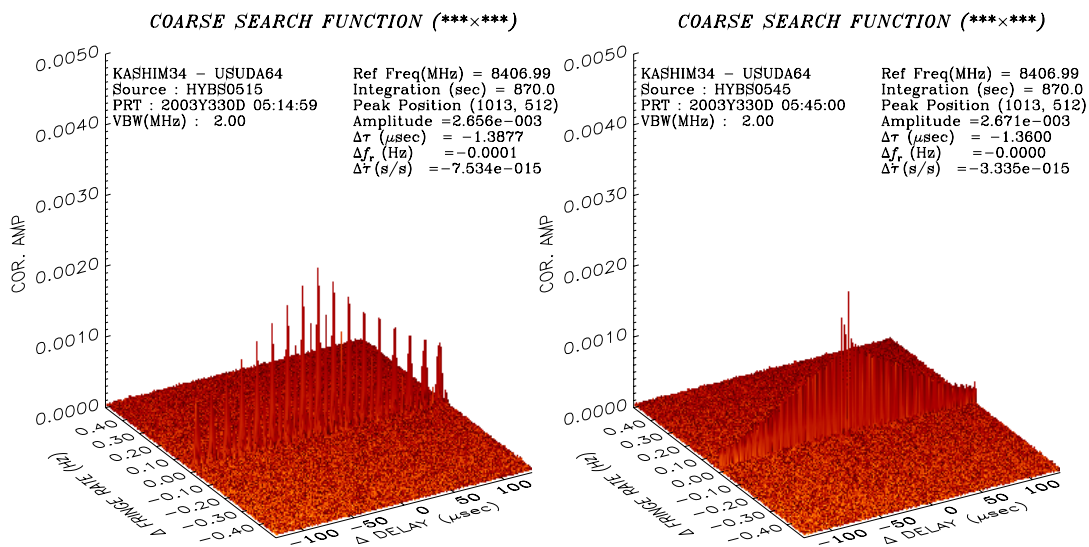


Figure 1. Detected HAYABUSA group delay fringes for the Kashima 34m – Usuda 64m baseline on November 26, 2003. (left: range signal, right: telemetry signal)

The large scattering of the group delays are shown at the first four epochs and after about 07:30UT in Figure 2. On the other hand, the relatively small scattering less than 10 nanoseconds are shown during the period between 05:00UT and about 07:30UT. It is considered that the difference between them is caused by the characteristic of the radio signals transmitted from HAYABUSA. The group delays with large residuals are obtained by the telemetry signal which has narrow band-width less than 1 MHz. The other group delays are obtained by the range signal which has band-width more than 1.5 MHz. To improve the signal to noise ratio of the telemetry-based group delays, we are now planning to apply the DBBC (Digital Baseband Converter) filtering technique to the original K5 data set [Tateuchi, 2004]. The advantage of using the DBBC technique is to be possible applying our state-of-art Gigabit VLBI system for the wide band-width data acquisition to the narrow band-width signal such a spacecraft signals. We will report this issue in another paper.

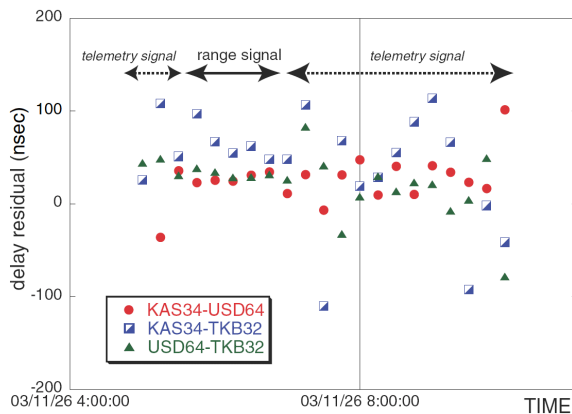


Figure 2. Residual delays between determined position using R&RR data by ISAS/JAXA and VLBI group delay observables.

References

- Ichikawa, R., M. Sekido, H. Osaki, Y. Koyama, T. Kondo, T. Ohnishi, M. Yoshikawa, and NOZOMI DVLBI group, An evaluation of VLBI observations for the positioning of the NOZOMI Spacecraft and the future direction in research and development of the deep space tracking using VLBI, *IVS CRL-TDC News No.23*, pp.31–33, 2003.
- JAXA web site, <http://www.muses-c.isas.jaxa.jp/English/index.html>, 2003.
- Kondo, T., Y. Koyama, R. Ichikawa, M. Sekido, and H. Osaki, Quasi real-time positioning of spacecrafts using the Internet VLBI system, *IUGG proceedings*, 2003.
- Sekido, M., R. Ichikawa, H. Osaki, T. Kondo, Y. Koyama, M. Yoshikawa, and NOZOMI VLBI observation group, VLBI application for spacecraft navigation (NOZOMI) –follow-up on model and analysis–, *IVS CRL-TDC News No.23*, pp.34–35, 2003.
- Takeuchi, H., Development of software baseband converter, *IVS NICT-TDC News No.24*, pp.9–10, 2004.

Development of Software Base-band Converter

Hiroshi Takeuchi (*ht@nict.go.jp*)

Kashima Space Research Center, National Institute of Information and Communications Technology, 893-1 Hirai, Kashima, Ibaraki 314-8501, Japan

1. Introduction

NICT has been developing software-based base-band converters which down-convert signals from broadband IF (intermediate frequency) to base-band using PC-based gigabit data acquisition system. While the DBBCs (Digital Base Band Converters) used in the conventional system consist of electric devices like FPGAs and ASICs, recent development of PCs enables us using PC software for the converter. By using PCs, simple and highly flexible system is expected to be realized at low cost.

2. System Configuration

The software-based BBC system consists of gigabit sampler ADS-1000 and a PC equipped with a PC-VSI data capture card and RAID hard disk drives [Kimura, et al., 2003]. IF-signals are sampled at the rate of 1Gpbs/2bit or 512Mbps/2bits by ADS-1000 and the sampled data are transferred to the memory in the PC via PC-VSI card (See Figure 1). When the baseband conversion is not necessary, obtained data are written to the hard

disk drives directly. When the BBC mode is on, data in the memory are filtered by band-pass filtering software and resulting data are written in real-time. The bandwidth of a resulting baseband data is selectable from 512kHz to 32MHz (data rates are twice than those). Quantization bits can be set from 1, 2, 4, and 8, and one or two baseband channels can be extracted in real-time with the PC. The band-pass filtering software is written in assembler language for the purpose of effective use of SSE/SSE2 function, which handles vector operations on x86 machines. It runs 10-times faster than that written in high-level languages like C and C++ language. An example of the frequency response of the system is shown in Figure 2.

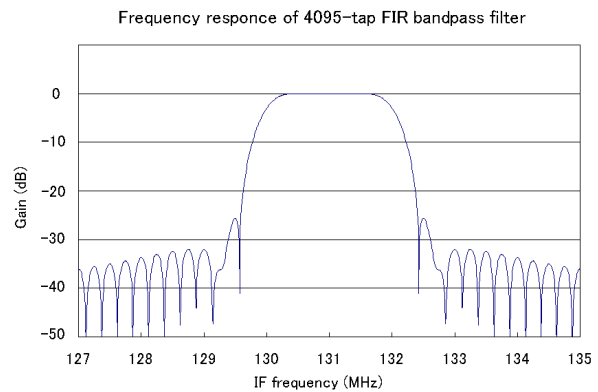


Figure 2. Frequency response of 4095-tap FIR band-pass filter, which generates 2-MHz bandwidth of baseband signals from 512-MHz bandwidth of IF-signals.

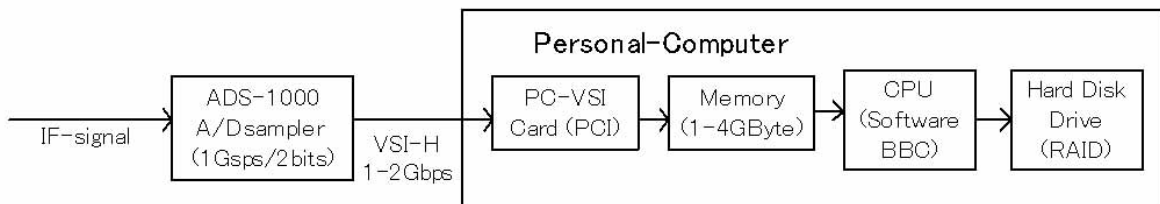


Figure 1. Schematic diagram of the software baseband converter system. Sampled VSI data are written not to HDDs (Hard Disk Drives) directly but to PC memory so that various kind of real-time data operations are possible before recording to the HDDs.

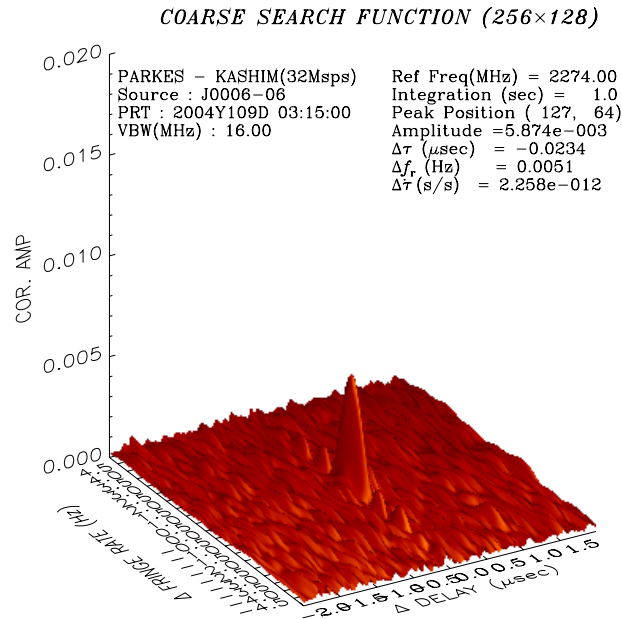


Figure 3. Detected fringe signals of J006-06 between Parks and Kashima.

3. Observational result

In order to evaluate the performance of the system, a VLBI experiment was performed between Kashima (Japan) and Parkes (Australia) VLBI stations on 18 April, 2004. At Kashima station, 256-MHz IF-signals were directly sampled and converted to 16-MHz signals by the software BBC system. At Parkes station, PC-EVN system was used for a data acquisition. A detected fringe signal is shown in Figure 3. The calculated correlation amplitude was confirmed to be reasonable compared to a value with the conventional system.

4. Future plan

We believe that this system will be a useful tool for differential VLBI observations for spacecraft navigations [Ichikawa *et al.*, 2004]. In the observations, target source is switched between spacecraft and phase-reference QSOs in order to cancel out phase variations. To prepare a sufficient number of phase-reference QSOs near the spacecraft, wide-bandwidth IF sampling is effective. On the other hand, DBBC is useful for the observations of spacecrafts because the bandwidth of the spacecraft signals is very narrow. Using the software BBC system, total data size can be reduced and the signal-to-noise ratio of the data can be improved for the narrowband spacecraft signals. Because the phase

relationship is preserved through the baseband conversion processes, we can use wideband quasar signals as phase reference for narrowband spacecraft signals.

Because the present system is based on the band-pass sampling method, selectable baseband frequencies are restricted. In more general cases, we should emulate the image rejection filter by using Hilbert filter, digital synthesizer and digital mixer. FPGA-based hardware system is suitable for the cases at present, but software-based system will also be usable in near future. The conventional multi-channel VLBI backend system will be able to be replaced with the system.

References

- Ichikawa, R., M. Sekido, H. Osaki, Y. Koyama, T. Kondo, M. Yoshikawa, and VLBI spacecraft tracking group, HAYABUSA VLBI Observations for Development of Deep Space Tracking –Preliminary Report–, *IVS NICT TDC News*, No.24, pp. 9–10, 2004.
- Kimura, M., J. Nakajima, H. Takeuchi, and T. Kondo, 2-Gbps PC Architecture and Gbps data processing in K5/PC-VSI, *IVS CRL-TDC News*, No.23, pp.12–13, 2003.

Derivation of relativistic VLBI delay model for finite distance radio source (Part I)

Mamoru Sekido¹ (*sekido@nict.go.jp*) and Toshio Fukushima²

¹*Kashima Space Research Center
National Institute of Information and
Communications Technology, 893-1 Hirai,
Kashima, Ibaraki 314-8501, Japan*

²*National Astronomical Observatory of Japan,
2-21-1 Osawa Mitaka Tokyo 181-8588, Japan*

Abstract: For the purpose to be used in correlation processing and data analysis of VLBI application in spacecraft navigation, relativistic VLBI delay model for finite distance radio source was developed. This delay model has precision of a pico second or better for any spacecraft including even low earth orbit satellite with 100km altitude. The formula of delay expression is in quite similar form with the consensus model, which is standard VLBI delay model. Thus it is relatively easy to be implemented in the current VLBI analysis packages. Detailed derivation procedure of the delay model is described in this paper (Part I). Delay rate and partial derivative with respect to radio source coordinates and station coordinates will be described in the paper part II in the next issue.

1. Introduction

Relativistic VLBI delay models had been actively discussed in the end of 1980s and beginning of 1990s. *Eubanks* [1991] has summarized those models as 'Consensus Model', and it is currently used in world wide VLBI community as a standard VLBI model. The consensus model uses plane wave approximation by assuming the radio source at infinite distance from observer. This assumption is valid for ordinary natural radio sources, which are farther distance than hundreds of light year away, in geodetic and astronomical VLBI observations. When VLBI technique is applied to radio sources at distance closer than 30 light years (e.g. planets, asteroids, and spacecraft in the solar system), however, the consensus model is not accurate enough and alternative relativistic VLBI delay model is required, since the curvature of wavefront need to be taken into account [*Sovers and Jacobs*, 1996]. *Fukushima* [1994] and *Sovers and Jacobs* [1996] discussed on VLBI delay mode for finite distance radio source, although a relativistic VLBI delay model corresponding to the consensus model was not proposed in those papers. *Moyer* [2000] derived VLBI

delay model based on light time (LT) solution for spacecraft navigation (hereafter LT-like approach). The LT requires iterative computation to solve it and it is different approach from that of conventional VLBI delay model. We preferred to use alternative formula corresponding to the consensus model (VLBI-like approach), so that it can easily be implemented in current VLBI analysis software. Additionally our VLBI-like approach may have advantage for distant radio source, because larger part of delays of two legs from spacecraft to observation stations are canceled out in LT-like approach as the radio source distance get farther.

We derive a relativistic VLBI delay model for finite distance radio source (hereafter finite-VLBI) by following the approaches of *Hellings* [1986], *Shahid-Saless and Hellings* [1991], and *Fukushima* [1994]. Relativistic delay model for finite-VLBI has already derived by *Sekido and Fukushima* [2004] with first order approximation. Although that approximation was valid when radio source is farther than 10^9 meters away. We describe a corrected and more detailed derivation procedure in this paper. The new formular derived here has precision better than 1 pico second for any spacecraft including low earth orbit satellites.

Derivation of relativistic VLBI delay model is described in this paper (part I), and time derivative and partial derivative of VLBI delay with respect to the radio source coordinates and station coordinates will be described in a article (Part II) in the next issue of IVS NICT-TDC news. Authors tried to describe rather detail of derivation procedure of formulae and modification of each equations, so that the derivation procedure is understandable and readers could follow the derivation.

Notation of variables used through out these articles are as follows. Variables of large Roman character indicate quantity in flat (Minkowskian) coordinate system of solar system barycenter (TCB-frame or TDB-frame, which are introduced later). Those of small Roman character indicates quantity in geocentric frame of reference and small Greek character means quantity on the geoid.

Most of variables used in this paper are listed as follows and subscript $i=0, 1, 2$, and E means respectively, 0:Radio source, 1: station-1, 2: station-2, and E : geocenter.

\vec{x}_i : Position vector of i in Solar System Barycenter (SSB) frame of reference (TCB-frame or TDB-frame).

\vec{x}_i : Position vector of i in geocentric coordinate frame of reference (hereafter TCG-frame), whose time like argument is Geocentric Coordinate Time (TCG).

$\vec{\xi}_i$: Position vector of i in local reference frame on the geoid, whose time like argument is Terrestrial Time (TT).

$\vec{\mathbf{R}}_{ij}$: Relative vector in the SSB frame of reference (TCB-frame or TDB-frame). $\vec{\mathbf{R}}_{ij} = \vec{\mathbf{X}}_i - \vec{\mathbf{X}}_j$

$\vec{\mathbf{r}}_{ij}$: Relative vector in the TCG-frame. $\vec{\mathbf{r}}_{ij} = \vec{\mathbf{x}}_i - \vec{\mathbf{x}}_j$

$\vec{\rho}_{ij}$: Relative vector in the TT-frame. $\vec{\rho}_{ij} = \vec{\xi}_i - \vec{\xi}_j$

$\vec{\mathbf{V}}_i$: Coordinate velocity vector of i in SSB frame of reference.

$\vec{\mathbf{w}}_i$: Coordinate velocity vector of i in the TCG-frame.

T_i : Coordinate time (TCB or TDB) in SSB frame of reference, when radio signal arrived at or departed from station i .

t_i : Coordinate time (TCG) in the TCG-frame, when radio signal arrived at station i .

τ_i : Proper time on the geoid (Terrestrial Time: TT), when radio signal arrived at station i .

c : Definition of speed of light: 299792458 m/s.

U_E : Gravitational potential at geocenter
 $U_E = \sum_{J \neq E} \frac{GM_J}{r_J}$

γ : One of the Post-Newtonian parameters and $\gamma = 1$ for general relativity.

γ_s : Lorentz Factor $1/\sqrt{1 - V^2/c^2}$

R_{ij} : Amplitude of vector $\vec{\mathbf{R}}_{ij}$. $R_{ij} = |\vec{\mathbf{R}}_{ij}|$

$\hat{\mathbf{R}}_{ij}$: Unit vector of $\vec{\mathbf{R}}_{ij}$. $\hat{\mathbf{R}}_{ij} = \frac{\vec{\mathbf{R}}_{ij}}{R_{ij}}$

β_{ij} : $\beta_{ij} = \hat{\mathbf{R}}_{ij} \cdot \frac{\vec{\mathbf{V}}_i}{c}$

β_i : $\beta_i = V_i/c$

Barycentric Coordinate Time (TCB) is the time like argument of Barycentric Coordinate Frame of reference (TCB-frame). Barycentric Dynamical Time (TDB) is the time like argument of Barycentric Dynamical Frame of reference (TDB-frame). Planetary coordinates in JPL Ephemeris are given in TDB-frame with time argument of TDB. Thus spacecraft coordinates are usually given in TDB, and here we also derive the delay model based on it. However, discussion based on TCB-frame is possible by setting scaling factor $L_B = 0$, which is introduced in the next section.

2. Coordinate Transformation

It is well accepted that linearized post Newtonian (post Galilean) metric

$$\begin{aligned} g_{00} &= 1 - 2\frac{U}{c^2} + O(c^{-4}) \\ g_{0k} &= O(c^{-3}) \\ g_{mn} &= -\delta_{mn}(1 + 2\gamma\frac{U}{c^2}) + O(c^{-4}) \end{aligned} \quad (1)$$

is appropriate to describe relativistic effects in moderate speed and gravitational field [Moyer, 2000; Hellings, 1986; Shahid-Sales and Hellings, 1991]. Infinitesimal line element of events scaled by a factor

$$l = 1 + L \quad (2)$$

is given as

$$ds^2 = l^2 \left[\left(1 - 2\frac{U}{c^2}\right) c^2 dT^2 - \left(1 + 2\gamma\frac{U}{c^2}\right) \sum_{i=1}^3 dX^i{}^2 \right], \quad (3)$$

where $U = \sum_j \frac{GM_j}{R_j}$ is gravitational potential at the position of interest, and G is gravitational constant. The summation is taken for all sources of gravitation. An interval of proper time $d\tau$ is related with the interval ds along its world line by

$$d\tau = \frac{ds}{c} \quad (4)$$

Substituting equations. (2) and (4) into (3), expanding and retaining terms to order of $1/c^2$ gives equation

$$\frac{d\tau}{dT} = 1 - \frac{U}{c^2} - \frac{V^2}{2c^2} + L, \quad (5)$$

where V is coordinate velocity of that point in SSB frame of reference. Scaling constant L is supposed to be order of $1/c^2$. When the point of interest is on the geoid, proper time τ become the Terrestrial Time (TT). Coordinate time T with the same rate with TT in average is realized by choosing the scale factor L appropriately. Supposing that long time average of equation (5) equals to unity when scaling constant $L = L_B$,

$$\langle \frac{d\tau}{dT} \rangle = 1 - \langle \frac{U}{c^2} + \frac{V^2}{2c^2} \rangle + L_B = 1. \quad (6)$$

Then scaling factor L_B is defined by

$$L_B = \frac{1}{c^2} \langle U + \frac{V^2}{2} \rangle, \quad (7)$$

where brackets $\langle \rangle$ means long time average. Currently, $L_B = 1.55051976772 \times 10^{-8} \pm 2 \times 10^{-17}$ is used as scaling factor [McCarthy and Petit, 2003]. The coordinate time scaled by $l = 1 + L_B$ is

the TDB and corresponding Barycentric Dynamical Frame of reference is defined by scaled metric by this factor.

By using gravitational potential at the geocenter $U_E = \sum_{J \neq E} \frac{GM_J}{r_J}$ and the scaling factor L_B , a new coordinates parameter of infinitesimal transformation can be defined.

$$dT' = (1 + L_B) \sqrt{1 - 2 \frac{U_E}{c^2}} dT \quad (8-a)$$

$$d\vec{X}' = (1 + L_B) \sqrt{1 + 2\gamma \frac{U_E}{c^2}} d\vec{X}. \quad (8-b)$$

By substituting equation (8) to (3), infinitesimal line element between events is expressed by

$$ds^2 = c^2 dT'^2 - \sum_{i=1}^3 dX'^i{}^2.$$

This means that the new parameters (dT' , $d\vec{X}'$) represent local Minkowskian flat coordinates system around the geocenter at that moment.

Now, geocentric local inertia coordinate system (dt , $d\vec{x}$) co-moving with geocenter and small portion of SSB frame around the geocenter expressed by (dT' , $d\vec{X}'$) can be transformed each other by Lorentz transformation, since both systems are local inertia frames.

$$cdt = \gamma_s cdT' - \gamma_s \frac{\vec{V}_E \cdot d\vec{X}'}{c} \quad (9-a)$$

$$d\vec{x} = d\vec{X}' + (\gamma_s - 1) \frac{\vec{V}_E \cdot d\vec{X}'}{V_E^2} \vec{V}_E - \gamma_s \vec{V}_E dT', \quad (9-b)$$

where V_E is coordinate velocity of earth evolution with respect to the SSB. And $\gamma_s = 1/\sqrt{1 - \frac{V_E^2}{c^2}}$ is Lorentz factor. Substituting equation (8) to (9), expanding, and retaining up to order of ($1/c^2$) becomes

$$\begin{aligned} dt &= \gamma_s(1 + L_B) \left(1 - \frac{U_E}{c^2}\right) dT \\ &\quad - \gamma_s(1 + L_B) \left(1 + \gamma \frac{U_E}{c^2}\right) \frac{\vec{V}_E \cdot d\vec{X}}{c^2} \\ &\cong \left(1 - \frac{U_E}{c^2} + \frac{V_E^2}{2c^2} + L_B\right) dT - \frac{\vec{V}_E \cdot d\vec{X}}{c^2} \end{aligned} \quad (10-a)$$

$$\begin{aligned} d\vec{x} &= (1 + L_B) \left(1 + \gamma \frac{U_E}{c^2}\right) d\vec{X} \\ &\quad + (1 + L_B)(\gamma_s - 1) \left(1 + \gamma \frac{U_E}{c^2}\right) \frac{\vec{V}_E \cdot d\vec{X}}{V_E^2} \vec{V}_E \\ &\quad - (1 + L_B) \left(1 - \frac{U_E}{c^2}\right) \gamma_s \vec{V}_E dT \\ &\cong \left(1 + \gamma \frac{U_E}{c^2} + L_B\right) d\vec{X} + \frac{\vec{V}_E \cdot d\vec{X}}{2c^2} \vec{V}_E \\ &\quad - \left(1 - \frac{U_E}{c^2} + \frac{V_E^2}{2c^2} + L_B\right) \vec{V}_E dT. \end{aligned} \quad (10-b)$$

These equations are the infinitesimal transformation between the Barycentric Dynamical Frame of reference (TDB-frame) and Geocentric Coordinates Frame of reference (TCG-frame). Inverse Lorentz transformation of equation (9) is

$$cdT' = \gamma_s cdt + \gamma_s \frac{\vec{V}_E \cdot d\vec{x}}{c} \quad (11-a)$$

$$d\vec{X}' = d\vec{x} + (\gamma - 1) \frac{\vec{V}_E \cdot d\vec{x}}{V_E^2} \vec{V}_E + \gamma_s \vec{V}_E dt. \quad (11-b)$$

Inverting equations. (8) by expanding and retaining terms in order of $1/c^2$ is

$$dT = \left(1 + \frac{U_E}{c^2} - L_B\right) dT' \quad (12-a)$$

$$d\vec{X} = \left(1 - \gamma \frac{U_E}{c^2} - L_B\right) d\vec{X}'. \quad (12-b)$$

Then infinitesimal inverse transformation from TCG-frame to TDB-frame in vicinity of the earth is given in order of c^{-2} as

$$dT = \left(1 + \frac{U_E}{c^2} + \frac{V_E^2}{2c^2} - L_B\right) dt + \frac{\vec{V}_E \cdot d\vec{x}}{c^2} \quad (13-a)$$

$$\begin{aligned} d\vec{X} &= \left(1 - \gamma \frac{U_E}{c^2} - L_B\right) d\vec{x} + \frac{\vec{V}_E \cdot d\vec{x}}{2c^2} \vec{V}_E \\ &\quad + \left(1 - \gamma \frac{U_E}{c^2} + \frac{V_E^2}{2c^2} - L_B\right) \vec{V}_E dt \end{aligned} \quad (13-b)$$

The scaling relation between TCG-frame (t, \vec{x}) and local reference frame on the geoid (hereafter referred as TT-frame) ($\tau, \vec{\xi}$) is given by

$$d\tau = (1 - L_G) dt \quad (14-a)$$

$$d\vec{\xi} = (1 - L_G) d\vec{x}, \quad (14-b)$$

where $L_G = \frac{W_g}{c^2}$ is scaling constant defined by gravitational potential W_g on the geoid, and its numerical value is defined as $L_G = 6.969290134 \times 10^{-10}$ [McCarthy and Petit, 2003]. Using equations (10), (13), and (14), and retaining terms in order of $1/c^2$ yields infinitesimal transformation from TDB-frame to TT-frame as

$$\begin{aligned}
d\tau &= \left(1 - \frac{U_E}{c^2} + \frac{V_E^2}{2c^2} + L_B - L_G\right) dT \\
&\quad - (1 - L_G) \frac{\vec{V}_E \cdot d\vec{X}}{c^2} \\
&\cong \left(1 - \frac{U_E}{c^2} + \frac{V_E^2}{2c^2} + L_C\right) dT - \frac{\vec{V}_E \cdot d\vec{X}}{c^2} \quad (15-a) \\
d\vec{\xi} &= \left(1 + \gamma \frac{U_E}{c^2} + L_B - L_G\right) d\vec{X} + \frac{\vec{V}_E \cdot d\vec{X}}{2c^2} \vec{V}_E \\
&\quad - \left(1 - \frac{U_E}{c^2} + \frac{V_E^2}{2c^2} + L_B - L_G\right) \frac{\vec{V}_E}{c} dT \\
&\cong \left(1 + \gamma \frac{U_E}{c^2} + L_C\right) d\vec{X} + \frac{\vec{V}_E \cdot d\vec{X}}{2c^2} \vec{V}_E \\
&\quad - \left(1 - \frac{U_E}{c^2} + \frac{V_E^2}{2c^2} + L_C\right) \frac{\vec{V}_E}{c} dT \quad (15-b)
\end{aligned}$$

and its inverse transformation

$$\begin{aligned}
dT &= \left(1 + \frac{U_E}{c^2} + \frac{V_E^2}{2c^2} - L_B + L_G\right) d\tau \\
&\quad + \left(1 + \frac{U_E}{c^2} + \frac{V_E^2}{2c^2} - L_B + L_G\right) \frac{\vec{V}_E \cdot d\vec{\xi}}{c^2} \\
&\cong \left(1 + \frac{U_E}{c^2} + \frac{V_E^2}{2c^2} - L_G\right) d\tau + \frac{\vec{V}_E \cdot d\vec{\xi}}{c^2} \quad (16-a) \\
d\vec{X} &= \left(1 - \gamma \frac{U_E}{c^2} - L_B + L_G\right) d\vec{\xi} + \frac{\vec{V}_E \cdot d\vec{\xi}}{2c^2} \vec{V}_E \\
&\quad + \left(1 - \gamma \frac{U_E}{c^2} + \frac{V_E^2}{2c^2} - L_B + L_G\right) \vec{V}_E d\tau \\
&\cong \left(1 - \gamma \frac{U_E}{c^2} - L_C\right) d\vec{\xi} + \frac{\vec{V}_E \cdot d\vec{\xi}}{2c^2} \vec{V}_E \\
&\quad + \left(1 - \gamma \frac{U_E}{c^2} + \frac{V_E^2}{2c^2} - L_C\right) \vec{V}_E d\tau, \quad (16-b)
\end{aligned}$$

where $L_C = L_B - L_G$ is used. In the same way, the relation between TCB-frame and TT-frame is easily obtained by placing $L_B = 0$. Actually replacement of $L_C \implies -L_G$ in equations. (15) and (16) give the infinitesimal transformations between TCB-frame and TT-frame. The TDB-frame is supposed as the SSB frame in the discussion in the following sections, however, the same discussion is valid for TCB-frame by the simple replacement of the scaling factor.

3. VLBI delay expression with Halley's formula

Let us suppose radio signal departed from radio source 0 at T_0 and arrive at observer 1 and 2 at epoch T_1 , and T_2 , respectively. Relative position vector from observer 2 at T_2 to the radio source 0

at T_0 is approximately expressed by relative vector $\vec{R}_{02}(T_1)$ and velocity vector \vec{V}_2 in the TDB-frame as follows:

$$\vec{R}_{02}(T_2) = \vec{R}_{02}(T_1) - \vec{V}_2(T_2 - T_1), \quad (17)$$

where acceleration of station 2 was eliminated. The time interval $T_2 - T_1$ is less than 42 milli-seconds on the ground baseline and acceleration contribution due to earth spin and evolution around the sun are $2.09 \times 10^{-2} m/s^2$ and 5.95×10^{-3} , respectively. Thus error of this approximation is less than 20 micro meters and negligible for our purpose. Square of this vector is

$$\begin{aligned}
R_{02}^2(T_2) &= R_{02}^2(T_1) - 2\vec{R}_{02}(T_1) \cdot \vec{V}_2(T_2 - T_1) \\
&\quad + V_2^2(T_2 - T_1)^2 \\
&= R_{02}^2 \left(1 - 2 \frac{\hat{\mathbf{R}}_{02} \cdot \vec{V}_2(T_2 - T_1)}{R_{02}} + \frac{V_2^2(T_2 - T_1)^2}{R_{02}^2}\right), \quad (18)
\end{aligned}$$

where $\vec{R}_{02}(T_1)$ is simply express by $\hat{\mathbf{R}}_{02}$ by eliminating the epoch in the second line. Taking square root and expanding it by Taylor series $\sqrt{1+x} = 1 + \frac{1}{2}x - \frac{1}{8}x^2 + \frac{1}{16}x^3 + \dots$ gives

$$\begin{aligned}
R_{02}(T_2) &= R_{02}(T_1) \left\{ 1 - \frac{\hat{\mathbf{R}}_{02} \cdot \vec{V}_2(T_2 - T_1)}{R_{02}} \right. \\
&\quad + \frac{V_2^2 - (\hat{\mathbf{R}}_{02} \cdot \vec{V}_2)^2}{2R_{02}^2} (T_2 - T_1)^2 \\
&\quad \left. + \frac{V_2^2 - (\hat{\mathbf{R}}_{02} \cdot \vec{V}_2)^2}{2R_{02}^3} (\hat{\mathbf{R}}_{02} \cdot \vec{V}_2) (T_2 - T_1)^3 + \dots \right\} \quad (19)
\end{aligned}$$

Retaining terms up to the 2nd order of $V_2(T_2 - T_1)$ becomes

$$\begin{aligned}
R_{02}(T_2) &= R_{02}(T_1) \left\{ 1 - \frac{\hat{\mathbf{R}}_{02} \cdot \vec{V}_2(T_2 - T_1)}{R_{02}} \right. \\
&\quad \left. + \frac{V_2^2 - (\hat{\mathbf{R}}_{02} \cdot \vec{V}_2)^2}{2R_{02}^2} (T_2 - T_1)^2 \right\}. \quad (20)
\end{aligned}$$

Truncation error of this approximation is order of $R_{02} \left(\frac{V_2(T_2 - T_1)}{R_{02}}\right)^3$ and this term increases as the distance R_{02} decreases. Magnitude of this term is less than 0.15 milli-meters in any spacecraft observations, even for low earth orbit satellite with 100 km altitude, for instance. In other words, this form has 1 pico second precision for any spacecraft in ground based interferometric observation. Time interval $T_2 - T_1$ can be expressed by using equation (20) as follows:

$$\begin{aligned}
c(T_2 - T_1) &= R_{02}(T_2) - R_{01}(T_1) + c\Delta t_g \quad (21) \\
&= c\Delta t_g - \vec{K} \cdot \vec{B} - \hat{\mathbf{R}}_{02} \cdot \vec{V}_2(T_2 - T_1) \\
&\quad + \frac{V_2^2 - (\hat{\mathbf{R}}_{02} \cdot \vec{V}_2)^2}{2R_{02}^2} (T_2 - T_1)^2, \quad (22)
\end{aligned}$$

where $\vec{\mathbf{K}}$ and $\vec{\mathbf{B}}$ is pseudo-source vector, which was introduced by *Fukushima* [1994] and baseline vector, which are defined in TDB-frame as

$$\vec{\mathbf{K}} = \frac{\vec{\mathbf{R}}_{01}(T_1) + \vec{\mathbf{R}}_{02}(T_1)}{R_{01}(T_1) + R_{02}(T_1)} \quad (23\text{-a})$$

$$\vec{\mathbf{B}} = \vec{\mathbf{X}}_2(T_1) - \vec{\mathbf{X}}_1(T_1). \quad (23\text{-b})$$

The pseudo-source $\vec{\mathbf{K}}$ vector correspond to the source vector in normal (infinite) VLBI model. But former is neither unit vector nor constant vector, whereas latter is constant unit vector. Δt_g is gravitational delay due to ray path bending. It is given by

$$\Delta t_g = (1 + \gamma) \sum_J \frac{GM_J}{c^3} \ln \left[\frac{(R_{0J} + R_{2J} + R_{20})(R_{0J} + R_{1J} - R_{10})}{(R_{0J} + R_{2J} - R_{20})(R_{0J} + R_{1J} + R_{10})} \right]. \quad (24)$$

An attention have to be paid to that radio source coordinates used in relative position vector $\vec{\mathbf{R}}_{0i}$ in above formulae are at the epoch T_0 , when the radio signal departed. Writing explicitly,

$$\vec{\mathbf{R}}_{0i}(T_1) = \vec{\mathbf{X}}_0(T_0) - \vec{\mathbf{X}}_i(T_1), \quad (i=1,2) \quad (25)$$

is used in following discussion in this paper. The epoch T_0 is obtained by solution of the following light time equation

$$T_1 - T_0 = \frac{|\vec{\mathbf{X}}_0(T_0) - \vec{\mathbf{X}}_E(T_1) - \vec{\mathbf{R}}_{1E}(T_1)|}{c} + (1 + \gamma) \sum_J \frac{GM_J}{c^3} \left(\frac{R_{0J} + R_{1J} + R_{10}}{R_{0J} + R_{1J} - R_{10}} \right). \quad (26)$$

Predicted orbit (position) of the radio source is supposed to be given as function of time. Position vector of station 1 $\vec{\mathbf{X}}_1 = \vec{\mathbf{X}}_E(T_1) + \vec{\mathbf{R}}_{1E}(T_1)$. Geocentric position vector $\vec{\mathbf{R}}_{1E}$ in TDB-frame is expressed by geocentric vector $\vec{\rho}_{1E}$ in TT-frame with equation (16) as

$$\begin{aligned} \vec{\mathbf{R}}_{1E} &= \left(1 - \gamma \frac{U_E}{c^2} - LC \right) \vec{\rho}_{1E} + \frac{\vec{\mathbf{V}}_E \cdot \vec{\rho}_{1E}}{2c^2} \vec{\mathbf{V}}_E \\ &+ \left(1 - \gamma \frac{U_E}{c^2} + \frac{V_E^2}{c^2} - LC \right) \vec{\mathbf{V}}_E d\Delta\tau_1^* \\ &= \left(1 - \gamma \frac{U_E}{c^2} - LC \right) \vec{\rho}_{1E} - \frac{\vec{\mathbf{V}}_E \cdot \vec{\rho}_{1E}}{2c^2} \vec{\mathbf{V}}_E. \end{aligned} \quad (27)$$

The second term of right hand side of the first line is due to difference of simultaneity between TDB-frame and TT-frame. Placing $dT = 0$, $d\vec{\mathbf{X}} = \vec{\mathbf{R}}_{1E}$

in equation (15-a), and retaining terms of $1/c^2$ order becomes

$$\Delta\tau_1^* = -\frac{\vec{\mathbf{V}}_E \cdot \vec{\mathbf{R}}_{1E}}{c^2} = -\frac{\vec{\mathbf{V}}_E \cdot \vec{\rho}_{1E}}{c^2}.$$

Relative vector $\vec{\mathbf{R}}_{1E}$ is computed with $\vec{\rho}_{1E}$ with equation (27). Position vector $\vec{\mathbf{X}}_0$ and $\vec{\mathbf{X}}_E$ is given as function of time from predicted orbit and planetary ephemeris. Equation (26) can be solved by iterative procedure such as Newton-Raphson method and initial value $T_0^{(0)} = T_1$.

To solve the equation (22) regarding $T_2 - T_1$, re-writing it by the order of $T_2 - T_1$ becomes

$$\begin{aligned} &\frac{V_2^2 - (\hat{\mathbf{R}}_{02} \cdot \vec{\mathbf{V}}_2)^2}{2R_{02}} (T_2 - T_1)^2 \\ &- (c + \hat{\mathbf{R}}_{02} \cdot \vec{\mathbf{V}}_2) (T_2 - T_1) \\ &+ c\Delta t_g - \vec{\mathbf{K}} \cdot \vec{\mathbf{B}} = 0. \end{aligned} \quad (28)$$

In general, when second order equation is given

$$\frac{1}{2} f'' x^2 + f' x + f^0 = 0, \quad (29)$$

approximation solution of it is known as

$$x = \frac{-f^0}{f' \left(1 - \frac{f^0 f''}{2f'^2} \right)}, \quad (30)$$

which is named Halley's formula. It becomes good approximation solution especially when $f'' f^0 \ll f'^2$, and this is the case. The other solution of the equation $x = \frac{-2f'}{f''}$ is rejected, since it is not obviously the solution of our interest.

Solution of equation (28) is expressed with Halley's formula as

$$T_2 - T_1 = \frac{\Delta t_g - \frac{\vec{\mathbf{K}} \cdot \vec{\mathbf{B}}}{c}}{(1 + \hat{\mathbf{R}}_{02} \cdot \frac{\vec{\mathbf{V}}_2}{c}) \left\{ 1 + \frac{\vec{\mathbf{K}} \cdot \vec{\mathbf{B}} \{ V_2^2 - (\hat{\mathbf{R}}_{02} \cdot \vec{\mathbf{V}}_2)^2 \}}{2c^2 R_{02} (1 + \hat{\mathbf{R}}_{02} \cdot \frac{\vec{\mathbf{V}}_2}{c})^2} \right\}}, \quad (31)$$

where term of $\Delta\tau_g$ in the denominator was eliminated because it is in order of c^{-4} . The solution is re-written by using $\beta_{02} = \hat{\mathbf{R}}_{02} \cdot \frac{\vec{\mathbf{V}}_2}{c}$ and $\beta_2 = V_2/c$ as

$$T_2 - T_1 = \frac{\Delta t_g - \frac{\vec{\mathbf{K}} \cdot \vec{\mathbf{B}}}{c}}{(1 + \beta_{02}) \left\{ 1 + \frac{\vec{\mathbf{K}} \cdot \vec{\mathbf{B}} (\beta_2^2 - \beta_{02}^2)}{2R_{02} (1 + \beta_{02})^2} \right\}} \quad (32)$$

Approximation error of Halley's formula is evaluated by $\frac{(f^0)^3 f''^2}{4f'^5} \simeq \frac{B}{4c} \left(\frac{B}{R_{02}} \right)^2 \beta^4$. This is in order of c^{-4} , thus it is safely negligible.

By the way, the relation of time interval $T_2 - T_1$ in TDB and $\tau_2 - \tau_1$ in TT is derived by using equation (16-a) as follows:

$$\begin{aligned}
T_2 - T_1 &= \left(1 + \frac{U_E}{c^2} + \frac{V_E^2}{2c^2} - L_C\right) (\tau_2 - \tau_1) \\
&\quad + \frac{\vec{\mathbf{V}}_E \cdot (\vec{\xi}_2(\tau_2) - \vec{\xi}_1(\tau_1))}{c^2} \\
&\cong \left(1 + \frac{U_E}{c^2} + \frac{V_E^2}{2c^2} - L_C\right) (\tau_2 - \tau_1) \\
&\quad + \frac{\vec{\mathbf{V}}_E \cdot [\vec{\mathbf{b}} + \vec{\mathbf{w}}_2(\tau_2 - \tau_1)]}{c^2} \\
&= \left(1 + \frac{U_E}{c^2} + \frac{V_E^2}{2c^2} + \frac{\vec{\mathbf{V}}_E \cdot \vec{\mathbf{w}}_2}{c^2} - L_C\right) \\
&\quad \times (\tau_2 - \tau_1) + \frac{\vec{\mathbf{V}}_E \cdot \vec{\mathbf{b}}}{c^2}, \tag{33}
\end{aligned}$$

where $\vec{\mathbf{b}} = \vec{\xi}_2(\tau_1) - \vec{\xi}_1(\tau_1)$ is baseline vector in TT-frame. $\vec{\xi}_2(\tau_2)$ is approximated as $\vec{\xi}_2(\tau_2) \cong \vec{\xi}_2(\tau_1) + \vec{\mathbf{w}}_2(\tau_2 - \tau_1)$, where $\vec{\mathbf{w}}_2$ is velocity vector in TCG-frame. Error of this approximation is less than 20 micro meters and negligible.

Relation between baseline vector in TDB-frame and TT-frame is derived with equation (16-b) as follows:

$$\begin{aligned}
\vec{\mathbf{B}} &= \vec{\mathbf{X}}_2(T_1) - \vec{\mathbf{X}}_1(T_1) \\
&= \left(1 - \gamma \frac{U_E}{c^2} - L_C\right) [\vec{\xi}_2(\tau_1^*) - \vec{\xi}_1(\tau_1)] \\
&\quad + \frac{\vec{\mathbf{V}}_E \cdot [\vec{\xi}_2(\tau_1^*) - \vec{\xi}_1(\tau_1)] \vec{\mathbf{V}}_E}{2c^2} \\
&\quad + \left(1 - \gamma \frac{U_E}{c^2} + \frac{V_E^2}{2c^2} - L_C\right) \vec{\mathbf{V}}_E(\tau_1^* - \tau_1) \\
&= \left(1 - \gamma \frac{U_E}{c^2} - L_C\right) [\vec{\mathbf{b}} + \vec{\mathbf{w}}_2(\tau_1^* - \tau_1)] \\
&\quad + \frac{\vec{\mathbf{V}}_E \cdot [\vec{\mathbf{b}} + \vec{\mathbf{w}}_2(\tau_1^* - \tau_1)] \vec{\mathbf{V}}_E}{2c^2} \\
&\quad + \left(1 - \gamma \frac{U_E}{c^2} + \frac{V_E^2}{2c^2} - L_C\right) \vec{\mathbf{V}}_E(\tau_1^* - \tau_1) \\
&\cong \left(1 - \gamma \frac{U_E}{c^2} - L_C\right) \vec{\mathbf{b}} - \frac{\vec{\mathbf{V}}_E \cdot \vec{\mathbf{b}}}{c^2} \left(\frac{\vec{\mathbf{V}}_E}{2} + \vec{\mathbf{w}}_2\right), \tag{34}
\end{aligned}$$

where terms in order of c^{-2} were retained. Time interval $\tau_1^* - \tau_1$ is due to difference of simultaneity between TDB-frame and TT-frame. Event at station 1 corresponds $(T_1, \vec{\mathbf{X}}_1) \Leftrightarrow (\tau_1, \vec{\xi}_1)$, and event at station 2 does $(T_1, \vec{\mathbf{X}}_2) \Leftrightarrow (\tau_1^*, \vec{\xi}_2)$. Thus $\tau_1^* - \tau_1$ is given by substituting $dT = 0$ in the equation (15-a) as

$$\tau_1^* - \tau_1 = -\frac{\vec{\mathbf{V}}_E \cdot \vec{\mathbf{B}}}{c^2} \cong -\frac{\vec{\mathbf{V}}_E \cdot \vec{\mathbf{b}}}{c^2} \tag{35}$$

Substituting equation (34) into (32) and retaining terms in order of c^{-2} becomes

$$\begin{aligned}
T_2 - T_1 &= \\
\Delta t_g - \left(1 - \gamma \frac{U_E}{c^2} - L_C\right) \frac{\vec{\mathbf{K}} \cdot \vec{\mathbf{b}}}{c} + \frac{\vec{\mathbf{V}}_E \cdot \vec{\mathbf{b}}}{c^3} \left(\frac{\vec{\mathbf{V}}_E}{2} + \vec{\mathbf{w}}_2\right) \cdot \vec{\mathbf{K}} \\
&\quad \frac{\Delta t_g - \left(1 - \gamma \frac{U_E}{c^2} - L_C\right) \frac{\vec{\mathbf{K}} \cdot \vec{\mathbf{b}}}{c} + \frac{\vec{\mathbf{V}}_E \cdot \vec{\mathbf{b}}}{c^3} \left(\frac{\vec{\mathbf{V}}_E}{2} + \vec{\mathbf{w}}_2\right) \cdot \vec{\mathbf{K}}}{(1 + \beta_{02})(1 + \alpha)}, \tag{36}
\end{aligned}$$

where following replacement of notation were used:

$$\beta_{ij} \stackrel{\text{def}}{=} \frac{\vec{\mathbf{R}}_{ij} \cdot \vec{\mathbf{V}}_j}{c} \tag{37-a}$$

$$\alpha \stackrel{\text{def}}{=} \frac{\vec{\mathbf{K}} \cdot \vec{\mathbf{b}}(\beta_2^2 - \beta_{02}^2)}{2R_{02}(1 + \beta_{02})^2} \tag{37-b}$$

$$\beta_2 \stackrel{\text{def}}{=} V_2/c. \tag{37-c}$$

Equating time interval of equations (36) and (33), solution of it with respect to $\tau_2 - \tau_1$ is

$$\tau_2 - \tau_1 = \frac{\Delta t_g - \left[1 - (\gamma + 1) \frac{U_E}{c^2} - \frac{V_E^2 + 2\vec{\mathbf{V}}_E \cdot \vec{\mathbf{w}}_2}{2c^2}\right] \frac{\vec{\mathbf{K}} \cdot \vec{\mathbf{b}}}{c} - \frac{\vec{\mathbf{V}}_E \cdot \vec{\mathbf{b}}}{c^2} [1 + \beta_{02} - \frac{(\vec{\mathbf{V}}_E + 2\vec{\mathbf{w}}_2) \cdot \vec{\mathbf{K}}}{2c}]}{(1 + \beta_{02})(1 + \alpha)}, \tag{38}$$

where pseudo-source vector $\vec{\mathbf{K}}$ is given by

$$\vec{\mathbf{K}} = \frac{\vec{\mathbf{R}}_{01}(T_1) + \vec{\mathbf{R}}_{02}(T_1)}{R_{01}(T_1) + R_{02}(T_1)}. \tag{39}$$

And these can be computed from observation station coordinates $(\vec{\rho}_{1E}(\tau_1), \vec{\rho}_{2E}(\tau_1))$ in TT-frame by

means of

$$\begin{aligned}\vec{\mathbf{R}}_{0i}(T_1) &= \vec{\mathbf{X}}_0(T_0) - \vec{\mathbf{X}}_1(T_1) \\ &= \vec{\mathbf{X}}_0(T_0) - \vec{\mathbf{X}}_E(T_1) - \vec{\mathbf{R}}_{iE}(T_1)\end{aligned}\quad (40-a)$$

$$\begin{aligned}\vec{\mathbf{R}}_{iE}(T_1) &= \left(1 - \gamma \frac{U_E}{c^2} - L_C\right) \vec{\rho}_{iE}(\tau_1) - \frac{\vec{\mathbf{V}}_E \cdot \vec{\rho}_{iE}}{2c^2} \vec{\mathbf{V}}_E. \\ &\text{, where (i=1,2).}\end{aligned}\quad (40-b)$$

Prediction orbit (position) of radio source ($\vec{\mathbf{X}}_0(T_0)$) and geocenter ($\vec{\mathbf{X}}_E(T_1)$) in TDB-frame are supposed to be given as function of time.

Equation (38) gives geometrical delay of VLBI measured by atomic clock on the geoid for finite distance radio source, when $\vec{\mathbf{X}}_0$ and $\vec{\mathbf{X}}_E$ is given in TDB-frame.

If radio source coordinates and earth ephemeris is given in TCB-frame, formula corresponding to equation (40-b) is obtained by replacing the scaling factor with $L_B \Rightarrow 0$ as

$$\vec{\mathbf{R}}_{iE}(T_1) = \left(1 - \gamma \frac{U_E}{c^2} + L_G\right) \vec{\rho}_{iE}(\tau_1) - \frac{\vec{\mathbf{V}}_E \cdot \vec{\rho}_{iE}}{2c^2} \vec{\mathbf{V}}_E, \quad (41)$$

where $i = 1, 2$.

Time derivative of delay (delay rate) and partial derivative with respect to radio source coordinates and station coordinates will be derived in the next paper (part II) in the next issue.

References

- Eubanks, T. M., A Consensus Model for Relativistic Effects in Geodetic VLBI, *Proc. of the USNO workshop on Relativistic Models for Use in Space Geodesy*, 60–82, 1991.
- Fukushima, T., Lunar VLBI observation model, *Astron. Astrophys.*, 291, 320–323, 1994.
- Hellings, R. W., Relativistic effects in astronomical timing measurements, *Astron. J.*, 91, 650–659, 1986.
- McCarthy, D. D. and G. Petit, IERS Conventions 2003, *IERS Technical Note*, No. 32, 2003
- Moyer, T. D., Formulation for Observed and Computed Values of Deep Space Network Data Types for Navigation, *JPL Monograph 2 (JPL Publication 00-7)*. This is published from *JPL Deep Space Communications and Navigation Series*, John Wiley & Sons. Inc., Hoboken New Jersey ISBN 0-471-44535-5, 2000
- Sekido M. and T. Fukushima, Relativistic VLBI delay model for finite distance radio source, Proceeding of IUGG 2003 in Sapporo, Special issued of J. of Geodesy, 2004 (in printing).
- Shahid-Saless, B. and R. W. Hellings, A Picosecond Accuracy Relativistic VLBI Model via Fermi Normal Coordinates, *Geophys. Res. Lett.*, 18, 1139–1142, 1991.

Sovers, O. J. and C. S. Jacobs, Observation Model and Parameter Partials for the JPL VLBI Parameter Estimation Software “MODEST”-1996”, *JPL Publication 83-39*, Rev. 6: 6–8, 1996.

The Australian experience with the PC-EVN recorder

Dodson, R^{1,2}, S. Tingay³, C. West³,
A. Hotan³, C. Phillips⁴, J. Ritakari⁵,
F. Briggs⁶, G. Torr⁶, J. Quick⁷,
Y. Koyama⁸, W. Brisken⁹, B. Reid²,
and D. Lewis⁴

¹ *Institute of Space and Astronautical Science,
JAXA, 3-1-1 Yoshinodai, Sagamihara,
Kanagawa 229-8510, Japan*

² *University of Tasmania, Hobart, 7000*

³ *Swinburne University of Technology,
PO Box 218, Hawthorn 3122, Melbourne,
Australia*

⁴ *Australia Telescope National Facility,
Commonwealth Scientific and Industrial
Research Organization, P. O. Box 76,
Epping NSW 2122, Australia*

⁵ *Metsähovi Radio Observatory,
Metsähovintie 114, 02540 Kylmälä, Finland*

⁶ *RSAA, The Australian National University,
Mount Stromlo Observatory, Cotter Road,
ACT 2611, Australia*

⁷ *Hartebeesthoek Radio Astronomy Observatory,
P.O. Box 443, Krugersdorp 1740, South Africa*

⁸ *Kashima Space Research Center, NICT,
893-1 Hirai, Kashima, Ibaraki 314-8501, Japan*

⁹ *National Radio Astronomy Observatory,
P.O. Box 0, Socorro, NM 87801, USA*

Abstract: We report on our experiences using the Metsähovi Radio Observatory's (MRO) VLBI Standard Interface (VSI, Whitney 2002) recorder in a number of astronomical applications. The PC-EVN device is a direct memory access (DMA) interface which allows 512 megabit per second (Mbps) or better recording to "off the shelf" PC components. We have used this setup to record at 640 Mbps for a pulsar coherent dispersion system and at 256 Mbps for a global VLBI session. We have also demonstrated recording at 512 Mbps and will form cross correlations between the CPSR-II and the PC-EVN systems.

1. Introduction

Astronomy has always battled against the extremely weak signals received from objects impossibly far away. We can improve the situation by recording the signals with cooler feeds, observing for longer, or by collecting wider bandwidths, as expressed by the radiometer equation (see e.g. Kraus 1986).

With modern digital technology it is possible to sample increasingly wider bandwidths with a higher number of bits. Furthermore by recording to consumer electronic hardware (the so called "Commercial off the Shelf" or COTS approach (e.g. Whitney 2003)) the equipment is cheap, reliable and easy to repair, replace and upgrade.

The potential downside of this is that everyone builds their own machine, with the equipment that was available at that moment (a particular problem with motherboards, which seem to have a lifetime of six months) and compatibility issues could arise. These, however, have not affected us and we have four very different configurations in use.

2. PC-EVN Hardware

The boards purchased from MRO were their two VSI boards; VSIB (a DMA card) and VSIC (a converter card). The VSIB card allows data to be written to or read from the hard drives on the PC. The provided operating system was debian linux (the stable woody series with kernel 2.4.19 and the big physical area patch). The recommended PC motherboard is the K7 series from MSI with an AMD processor. With these we run four IDE disks (200 GBytes in size) from the motherboard. A boot disk (and CD) is run from a PCI IDE card, making the total disk capacity one terabyte. The data disks are mounted in a (software) RAID0 array. We have also used the Dell 1600C server machine, because with these the data disks can be external Apple Xraid disks on a 64 bit PCI bus. These were run using SuSe 8.2 linux OS. Using alternate motherboards and OS versions caused no problems.

The cards cost €565 each, the PC the order of AU\$2000 and about the same for four 200 Gbyte hard drives. Therefore the total cost of the system was around AU\$5500.

3. The Mt. Pleasant Pulsar backend

Hobart has been monitoring the Vela pulsar's pulse time of arrival (TOA) for over twenty years. The original system (which caught a glitch in the first week of operation (McCulloch et al., 1983)) has been upgraded over the years to one that;

- monitors Vela for 18 hours a day (and a second glitching pulsar for the remaining 6 hours).
- collects two minute averaged profiles at three frequencies (635, 990 and 1390 MHz). The bandwidth is matched to the dispersion time for a dispersion measure (DM) of 69 pc cm⁻³. The automatically generated fit to these data is available on the web¹.

¹<http://www-ra.phys.utas.edu.au/~rdodson/0835-4510.par>

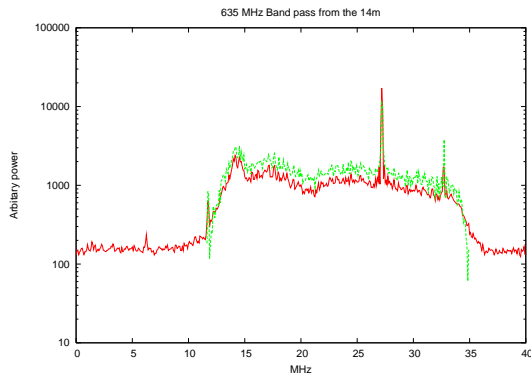


Figure 1. Autocorrelation of the 635 MHz band-pass. The interference around 27 MHz (637 MHz) can be excised in the profile formation. Both XF (red) and FX (green) correlator outputs are shown.

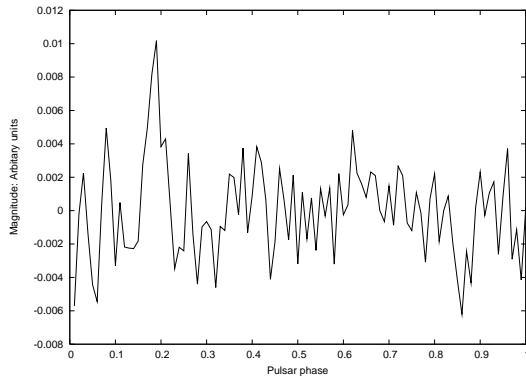


Figure 2. Profile of Vela from 0.7 second of data at 619 to 644 MHz.

- collects continuously sampled data at 990 MHz (incoherently dedispersed to increase the bandwidth by a factor of eight). From this single pulse system 10 second profiles are constantly formed and checked for the occurrence of a glitch. These data are saved for 3 days for deep analysis of immediate post (and pre) glitch behaviour (Dodson, McCulloch & Lewis 2002).
- now also collects continuous sampled data at 635 MHz across a 25 MHz bandpass offset from baseband by 10 MHz, increasing the bandwidth one hundred fold. This data is buffered for 2.5 hours, after which it is overwritten. Once a glitch is detected by the single pulse system the data is saved for off-line coherent dedispersion and profile forming.



Figure 3. The VLBI system with 4 demountable 200GB IDE drives.

The last Vela glitch (January 2000) spun-up the pulsar within the detection time of the single pulse system (i.e. less than 30 seconds) and also showed a previously undetected decaying spin-down term with a time constant of 1 minute (Dodson et al., 2002). Our new system will produce TOA's with accuracy of the order of 0.1 msec every second (as opposed to every 10 seconds with the single pulse or 120 seconds with the multi-frequency systems).

The IF (baseband to 40 MHz) was fed in to a MAXIM 1448 A/D mounted on an evaluation card (AU\$330 each), along with a 80 MHz clock. Two of these provide the two polarisations. The output of these are TTL, so the four most significant bits (of the 10 bits provided by the MAX1448 card) are buffered to LVDS along with the clock signal, and combined with an external 1PPS signal. These are fed directly into the VSIB. The recovered band-pass is shown in Figure 1. In running the VSIB at 80 MHz we are clocking the data at two and a half times the VSI standard, nevertheless this produced no complications. The recording software is that provided (**wr**), with minor modifications to allow continuous looped recording and shared memory control. This system is now running and recording data, and we are just waiting for the next glitch.

Once we have data covering the glitch event we will excise the interference, coherently dedisperse the signal, form 1 second profiles and measure the TOAs. This will be done with the ATNF/Swinburne software package PSRCHIVE (Hotan et al., 2004). The profile from a short section of data is shown in Figure 2.

4. The VLBI system

The VSIC card converts many "legacy" VLBI digital signals into the ordering and levels (LVDS)

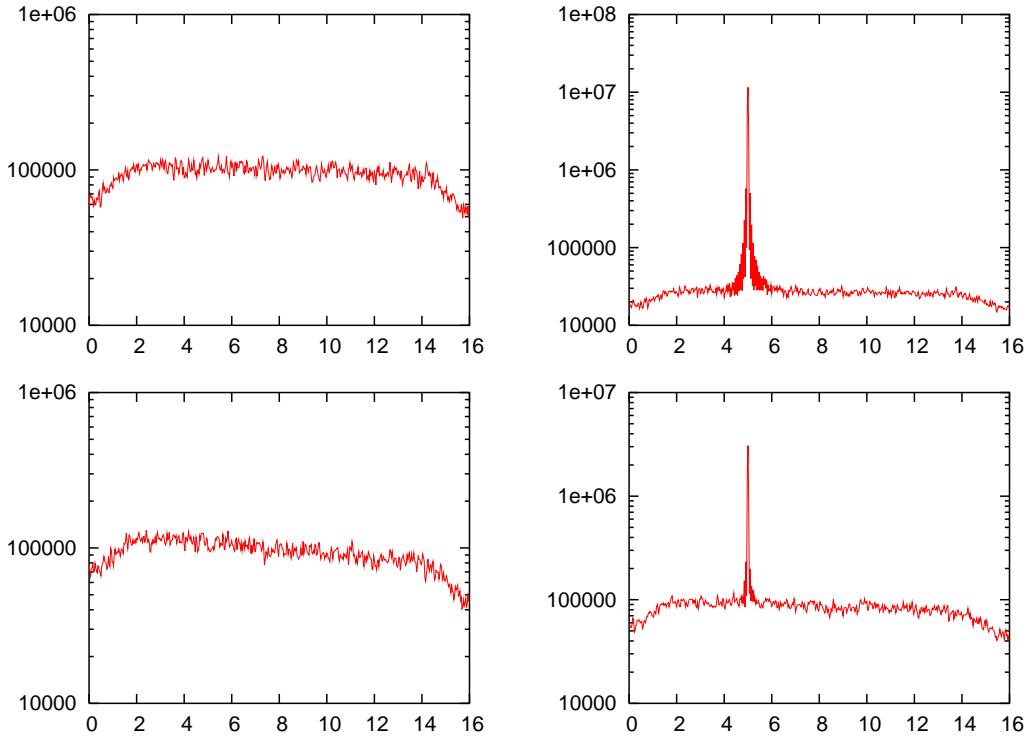


Figure 4. Autocorrelation of four 16MHz bandpasses (LHC and RHC at 4792-4808 and 4808-4824 MHz) from the ATNF DAS recorded on to the PC-EVN system. A LHC tone at 4797 MHz was injected.

of the VSI standard required by the VSIB DMA card. In the Hobart system the VSIC card is mounted and powered inside the PC case (see Figure 3, the connector is on the right under the hard drives). For the Swinburne systems the VSIC card was enclosed in its own box. The card will handle up to 32 channels of data, plus the required signal clocks and 1PPS signals.

The VSIC card will format data with S2 pin outputs (as well as VLBA, Mk3 and Mk4 formats), so it was a trivial task to connect the VSIC to the cable normally going to the S2 recorder. Once again the provided program `wr` was used to collect the data. `wr` reads a minimum of 8 channels, whilst the maximum rate S2 recording modes (32x4-2) records two IFs of 16 MHz of data at 2 bits into 4 channels. The DAS modes used (VSOP and MP16S), however, encode four IFs of 16 MHz of data at 2 bits into 8 channels. Therefore we could record double the usual LBA bandwidth using the PC-EVN system. Four 16 MHz bandpasses are shown in Figure 4. More details can be found in Dodson 2004.

The experiment performed was a global eVLBI observation. Most Australian telescopes (**ATCA**, **Mopra**, **Parkes**, **Tidbinbilla** and **Ceduna**) recorded on PC-EVN machines, and **Hobart**

recorded to their Mk5a system. Also recording on Mk5 systems were **Hartebeesthoek** (SA) and **Pietown** (USA). Data was recorded to the K5 system at **Kashima** in Japan.

During the experiment small sections of the recorded data from Ceduna, Mopra, Parkes, Tidbinbilla and Narrabri were transferred to various software correlators to perform near real time fringe checking. Various approaches to correlation have been developed; a XF and then fringe rotate correlator running on the Swinburne supercomputer, this is the correlator which we are planning to use for stage one VLBI data production. We also have test correlators running on a conventional PC which take various other approaches; FX then fringe rotate, XF then fringe rotate and a fringe rotate and XF correlator. For a 1 kHz channel width (which is equivalent to 0.2 km s^{-1} for 1.4 GHz) the fringe rotation needs to be less than 28 Hz to keep the phase change to less than 10° in a single integration period. This condition is fulfilled (so we can correlate then rotate) for the ATNF antennae (i.e. Parkes, Mopra and ATCA), but not for the more distant ones. However for continuum observations with a limited field of view the channel widths can be a thousand times greater, and the condition is met for all non-space base-

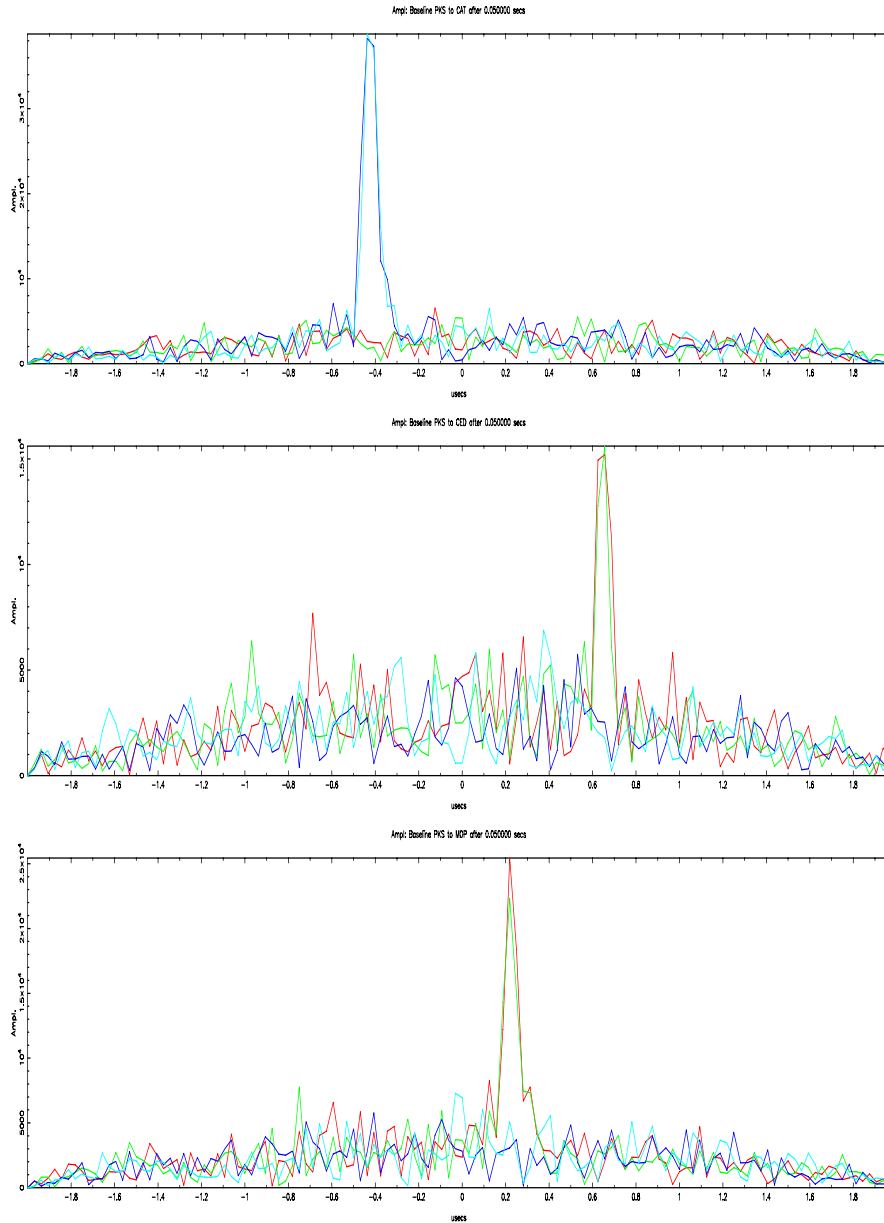


Figure 5. 0.1 second integrated cross correlation of four telescopes with PC-EVN systems on the strong continuum source J0006-0623 using 16 MHz centred at 2282 MHz. The fringes for Parkes to ATCA are in the cross hands (therefore in different colours) showing that the polarisations were swapped (Left and Right, rather than Right and Left) at that telescope.

lines. The major advantage of the XF then rotate mode is that we perform both the bit decoding and correlation calculation in a single lookup table operation. These rapid integer operations are seven times faster than the rotate and XF correlate method.

We observed the strong continuum sources J0006-0623, J1037-2934 and the pulsar Vela.

Fringes were found only two minutes after the wavefront reached the antennae using the Swinburne correlator. Figure 5 shows the delays found for Parkes to the ATCA, Ceduna and Mopra on J0006-0623 from the single processor correlator (in the XF & fringe rotate mode).

The data has now been transported on external disks to Swinburne to be correlated on the super-

computer. A full report on the software correlator, the experiments and the results is in preparation. Of particular note is that this is the first mixed format global eVLBI experiment.

5. The Stromlo Streamer

For radio astronomers, the radio frequency interference (RFI) environment continues to get worse, and has become a critically important issue in the development of the next generation of radio telescopes, including the Square Kilometre Array. For the SKA site evaluations and interference mitigation investigations Mount Stromlo Observatory (Australian National University) has used a near identical setup to the pulsar system as a flexible test bed for emulating radio astronomy backends in software. The system is portable, carrying with it a low-precision 64 MHz clock and 4 MAXIM 1448 A/D cards for accepting 4 IFs as input. The flexibility provided by the MRO `wr` routine allows the A/Ds to deliver different numbers of bits precision and different sampling rates without reconfiguring the hardware.

The most often used application has been in the area of RFI mitigation to further the program described in Briggs, Bell and Kesteven (2000). The four input channels can record, for example, the signals from two polarizations of a telescope as well as the signals from RFI sensors that are optimized to provide gain directed at broadcast towers. The ‘Streamer’ has seen action at Molonglo at 843 MHz, where the phased signals from East and West arms are recorded separately, along with RFI reference signals from both polarizations of a 6 m parabola. In these experiments, we recorded four 8 MHz bands with 8 bit precision and computed the cross-power spectra as well as total power spectra from all channels as a step toward RFI characterization and cancellation. We are exploring the implementation of similar techniques with the Swinburne CPSR-II system at Parkes, which can record twice the bandwidth of the PC-EVN system (i.e. four 64 MHz bandwidths). CPSR-II has the great additional benefit of 30 dual CPU processors, so that it is a production machine capable of doing the signal processing in real time, while the Streamer’s strong points are its portability, low cost and availability.

6. The future

Using the PC-EVN systems in place we will collect the data from the S2 formatter output port (C2a), and fringe check the data on the fly during all VLBI observations. Automation of the data collection is being organised.

We have collected the data from the DAS correlator port rather than the S2 connector port, which allows us to record 2 IFs of 64 MHz (at 2 bits). At Parkes we will use coincident data recorded on the CPSR-II system to produce the zero baseline cross correlations. We will shortly attempt to correlate CPSR-II data (from Parkes) with data from two PC-EVN machines (at ATCA) to demonstrate 1 Gbps VLBI in Australia. We are also investigating the possibility of using the system as a data buffer on the to-be-upgraded ATNF network (i.e. on the 10 Gbps links between antenna).

The recording rate limitations are from that sustainable by the hard drives (about 800 MBs), however when greater speeds are possible (with Serial IDE drives or just general improvements) we will be at the PCI maximum rate (1056 Mbs). Already we’d like to be able to read and write over the same bus at the same time, in which case developing the VSIB card to run on the faster, emerging, technologies would be of great priority. The estimated cost for this is 3 man months, and if sufficient interest is generated this will be undertaken at Metsähovi.

7. Conclusions

We have demonstrated the adaptability of the PC-EVN system, and its low cost of setup in both hardware and manpower. We have used it for analog RF recording systems and as a digital recorder for the Australian VLBI system.

References

- Briggs, F. H., J. F. Bell, and M. J. Kesteven, *Astron. J.*, 120, pp.3351–3361, 2000.
- Dodson, R., eLBA memo series, 1, 2004.
- Dodson, R. G., P. M. McCulloch, and D. R. Lewis, *Astrophys. J.*, 564, pp.L85–L88, 2002.
- Hotan, A. W., W. van Straten, and R. N. Manchester, *astro-ph/0404549*, 2004.
- Kraus, J. D., *Radio astronomy*, Powell, Ohio: Cygnus-Quasar Books, 1986.
- McCulloch, P. M., P. A. Hamilton, G. W. R. Royle, and R. N. Manchester, *Nature*, 302, pp.319-321, 1983
- Whitney, A., in e-VLBI workshop at JIVE, Parsley S., Whitney A., eds, Mark 5 and e-VLBI, 2003.
- Whitney, A., in e-VLBI workshop at Haystack, Parsley S., Whitney A., eds, VSI-H, 2003.

- News -

CARAVAN-35, Small Radio Telescope Package Released

Junichi Nakajima (*nakaji@nict.go.jp*)

*Kashima Space Research Center
National Institute of Information and Communications Technology
893-1 Hirai, Kashima, Ibaraki 314-8501, Japan*

CARAVAN 35 is a new portable educational radio telescope package (Figure 1). The minimum size 35-cm dish aperture is mainly targeting daytime Sun radio emission and users can understand radio telescope function from the simplified system. NICT (former CRL) had been held summer science course for high-school students. In this course, students can build their own radio telescope from scratch. Though we received strong demands to carry out this radio telescope education in high-school, often there is difficulty in school facility where they does not have microwave and electronic instruments.

For such educational purpose, we have designed RFD-1500 (Figure 2). The pocket sized total-power telescope backend includes microwave IF amplifier, splitter, detector and DC amplifier. Since the integrated RFD1500 succeeded to eliminate unstable behavior in high-Gain system, simply hook up the RFD1500 unit between satellite dish and DVM, student and teacher without microwave electronics background can perform experiment in short time. Starting from measuring antenna temperature, students learn Y-factor method, Solar temperature in satellite-band (10GHz), and telescope efficiency. Find fixed satellite in GSO orbit and following Sun in the sky help understanding of celestial coordinate system.

CARAVAN is named after our small VLBI telescope research project CARAVAN (Compact Antenna of Radio Astronomy VLBI Adapted Network). These VLBI dishes are 65-cm and 2.4m. In future we hope interferometric connection to the 35-cm little brothers in educational field.

CARAVAN-35 package include TDK TA-352 prime focused satellite dish, RFD-1500 radio telescope backend, high precision SANWA DVM, calibration blackbody absorber and accessories. The basic package is priced from 400USD. These are distributed from Electro Design Corporation (EDC). For further information please contact (Electro Design Co.Ltd., Nakane 169-2 Noda-city CHIBA JAPAN 278-0031 TEL81-4-7123-9511 FAX81-4-7123-9513, *skinoshita@edco.jp*)



Figure 1. CARAVAN-35 package is being distributed from EDC. 35- cm dish, RFD-1500 backend and DVM are the key components. By using RS-232 / USB readout of DVM, students can experience pen-recorder type basic observation essential in radio-astronomy.

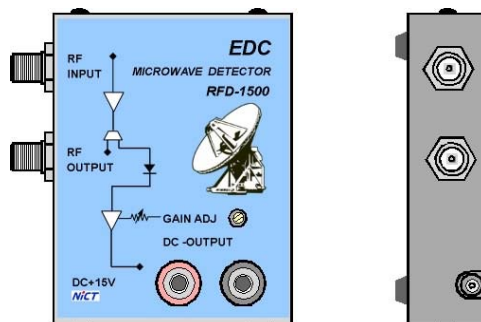


Figure 2. RFD1500, compact total-power backend. RF amplifier, detector and DC amplifier are packed into a small package. Student hook up satellite dish and RFD1500. Then the dish is transform into their own radio telescope.

“IVS NICT Technology Development Center News” (IVS NICT-TDC News) published by the National Institute of Information and Communications Technology (NICT) (former the Communications Research Laboratory (CRL)) is the continuation of “IVS CRL Technology Development Center News” (IVS CRL-TDC News). (On April 1, 2004, Communications Research Laboratory (CRL) and Telecommunications Advancement Organization of JAPAN (TAO) were reorganized as “National Institute of Information and Communications Technology (NICT)”.)

VLBI Technology Development Center (TDC) at NICT is supposed

- 1) to develop new observation techniques and new systems for advanced Earth’s rotation observations by VLBI and other space techniques,
- 2) to promote research in Earth rotation using VLBI,
- 3) to distribute new VLBI technology,
- 4) to contribute the standardization of VLBI interface, and
- 5) to deploy the real-time VLBI technique.

The NICT TDC newsletter (IVS NICT-TDC News) is published biannually by NICT.

This news was edited by Tetsuro Kondo and Yasuhiro Koyama, Kashima Space Research Center, who are editorial staff members of TDC at the National Institute of Information and Communications Technology, Japan. Inquires on this issue should be addressed to T. Kondo, Kashima Space Research Center, National Institute of Information and Communications Technology, 893-1 Hirai, Kashima, Ibaraki 314-8501, Japan, TEL : +81-299-84-7137, FAX : +81-299-84-7159, e-mail : kondo@nict.go.jp.

Summaries of VLBI and related activities at the National Institute of Information and Communications Technology are on the Web. The URL to view the home page of the Radio Astronomy Applications Section of the Kashima Space Research Center is : “<http://www.nict.go.jp/ka/radioastro/>”.

IVS NICT TECHNOLOGY DEVELOPMENT CENTER NEWS No.24, July 2004

International VLBI Service for Geodesy and Astrometry
NICT Technology Development Center News
published by

National Institute of Information and Communications Technology, 4-2-1 Nukui-kita, Koganei,
Tokyo 184-8795, Japan

